Singlet–Singlet Annihilation Kinetics in Aggregates and Trimers of LHCII

V. Barzda,*† V. Gulbinas,† R. Kananavicius,† V. Cervinskas,† H. van Amerongen,* R. van Grondelle,* and L. Valkunas†

*Faculty of Sciences, Department of Physics and Astronomy, Vrije Universiteit, 1081 HV Amsterdam, The Netherlands and †Institute of Physics, LV2600 Vilnius, Lithuania

ABSTRACT Singlet–singlet annihilation experiments have been performed on trimeric and aggregated light-harvesting complex II (LHCII) using picosecond spectroscopy to study spatial equilibration times in LHCII preparations, complementing the large amount of data on spectral equilibration available in literature. The annihilation kinetics for trimers can well be described by a statistical approach, and an annihilation rate of $(24\ \text{ps})^{-1}$ is obtained. In contrast, the annihilation kinetics for aggregates can well be described by a kinetic approach over many hundreds of picoseconds, and it is shown that there is no clear distinction between inter- and intratrimer transfer of excitation energy. With this approach, an annihilation rate of $(16\ \text{ps})^{-1}$ is obtained after normalization of the annihilation rate per trimer. It is shown that the spatial equilibration in trimeric LHCII between chlorophyll *a* molecules occurs on a time scale that is an order of magnitude longer than in Photosystem I-core, after correcting for the different number of chlorophyll *a* molecules in both systems. The slow transfer in LHCII is possibly an important factor in determining excitation trapping in Photosystem II, because it contributes significantly to the overall trapping time.

INTRODUCTION

In photosynthesis, two ultrafast processes underlay the high efficiency: energy transfer in the light-harvesting antenna (LHA) and charge separation in the reaction center (RC) (Dau, 1994; van Grondelle et al., 1994). A highly organized network of membrane-associated pigment–proteins constitutes the photosynthetic apparatus and its cooperativity is a key element (Dau, 1994; van Grondelle et al., 1994). Photosystem II (PSII) of green plants is probably the most intriguing photosynthetic system known today. Its primary electron donor, P680, has an extremely high redox potential, providing the system with the capability to split water, giving rise to the release of oxygen. Moreover, PSII is able to adapt to varying light conditions via nonphotochemical quenching mechanisms (for review see Horton et al., 1996). Recently, it was shown that a few minutes after dissolving thylakoid membranes in the detergent *n*-dodecyl α-D-maltoside (α-DM), PSII is organized in many different ways, revealing mutual contacts between trimers of light-harvesting chlorophyll (Chl) *a*/*b* pigment–protein complexes of PSII (LHCII), and contacts with minor light-harvesting complexes and the core of PSII, and it was argued that the differences in organization also occur in vivo (Boekema et al., 1995, 1998, 1999a,b). A further important finding was the contiguous arrangement of different PSII units (Boekema et al., 1999a), again showing contacts between LHCII trimers. Connectivity between the RCs of PSII units was already revealed from spectroscopic studies in 1976 (Paillotin, 1976). Fluorescence-induction measurements also showed that different RCs are connected in the thylakoid membrane, which leads to the description in terms of a lake model (Dau, 1994; Valkunas et al., 1992a). A connected units model was introduced by Lavergne and Trissl (1995). Connectivity of the antenna has to be taken into account, for instance, for correct modeling of the quenching of excitations by triplet states in thylakoid membranes (Sonneveld et al., 1979, 1980; Breton et al., 1979; Kolubayev et al., 1985) and for the fluorescence induction determined by the closure of the RCs (Paillotin et al., 1983). Recently, with the use of electron microscopy, paired grana membrane fragments were studied, and a rather common semi-regular array of supercomplexes was observed, consisting, on average, of 2 PSII core complexes and 3 LHCII trimers, in addition to the minor Chl *a*/*b* binding proteins (Boekema et al., 2000). The analysis suggested that many PSII–LHCII supercomplexes in one membrane face exclusively LHCII in the other. The possible existence of LHCII-only domains in the thylakoid membranes was corroborated by the structural characterization of a supramolecular complex, consisting of seven trimeric LHCII complexes (Dekker et al., 1999).

Numerous studies have been performed to elucidate the dynamics of light harvesting and charge separation in PSII (for reviews see van Grondelle, 1985; van Grondelle et al., 1994) leading to a large variation in results, possibly related to the above-mentioned variability and connectivity. The most extensive data set was collected for intact pea chloroplasts by Roelofs et al. (1992), and global lifetime analyses indicated PSII lifetimes of 290 and 630 ps for open RCs. The data were interpreted in terms of heterogeneity of PSII and the kinetics were explained with the exciton–radical pair equilibrium model (Roelofs et al., 1992), which is a member of the group of "trap-limited" models that have

Received for publication 19 July 1999 and in final form 5 February 2001.

Address reprint requests to Virginijus Barzda, University of California, San Diego, Dept. of Chemistry and Biochemistry, 9500 Gilman Dr., La Jolla, CA 92093. Tel.: 858-534-0290; Fax: 858-534-7654; E-mail: vbarzda@ucsd.edu.

0006-3495/01/05/2409/13 $2.00

been proposed in literature. However, also "diffusion-limited" models have been proposed by others (Butler et al., 1983; Berens et al., 1985a, 1985b). A third type of model, which seems to be applicable to chromatophores of purple bacteria, is the "transfer-to-trap limited" model (Valkunas et al., 1992b; Somsen et al., 1994, 1996). At this moment, none of the models has been commonly accepted for PSII. The essential difference between the various models can be understood as follows. The lifetime τ_{exc} of an excitation in a photosynthetic unit (RC + LHA) can be written as (Kudzmauskas et al., 1983; Valkunas, 1986; Valkunas et al., 1991)

$$\tau_{exc} = \tau_{trap} + \tau_{del} + \tau_{mig}, \quad (1)$$

where τ_{trap} is the trapping time, which is equal to the charge separation time τ_{cs} divided by the probability to find the excitation on the primary donor and not on one of the other pigments. In case the primary donor and all antenna pigments are isoenergetic (N pigments in total) one finds $\tau_{trap} = N\tau_{cs}$. If the total lifetime τ_{exc} is dominated by τ_{trap} then the process is trap-limited. The next term, τ_{del}, corresponds to the transfer between the LHA and the RC, but we will not further discuss it here. If this transfer step is rate limiting, the transfer-to-trap limited model can be applied. Finally, if the migration term, τ_{mig}, dominates, the trapping process is diffusion limited. For a regular lattice this term is given by $\tau_{mig} = 0.5Nf_d(N)W_h^{-1}$, where W_h is the hopping rate for excitations from one pigment to a neighboring one. The structure function $f_d(N)$ depends, not only on the number of pigments, but also on the actual arrangement of the pigment lattice, but its value is typically between 0.5 and 1 when the lattice contains on the order of 100 pigments or more (Kudzmauskas et al., 1983; Somsen et al., 1996). It is important to note that τ_{mig} scales almost linearly with N. Some deviation from linearity is caused by the influence of $f_d(N)$, but for large values of N ($\sim$100), the deviation is small (Pearlstein, 1982; Kudzmauskas et al., 1983; Valkunas, 1986). Therefore, when a trap-limited model is used, the assumption is made that the rate of charge separation (τ_{cs}^{-1}) from the primary donor is much slower than the average hopping rate for excitations. However, no consensus exists so far, neither about the value of τ_{cs} or about τ_{mig} (see e.g., van Grondelle et al., 1994). Important is the fact that PSII forms an energetic funnel toward the RC, which is only very shallow (Jennings et al., 1993), and, in all existing models, reversible transfer between the outer antenna and the core is (and should be) taken into account.

In principle, one can obtain information about τ_{mig} by studying the LHA separately. The LHA of PSII consists to a large extent of the main complex LHCII. Approximately 4 trimeric LHCIIs are present per RC (Jansson et al., 1997), and these are present in different arrangements (see above). A monomeric subunit of LHCII binds 5–6 Chl *b* molecules and 7–8 Chl *a* molecules, and 60% of the Chl *a* molecules and 90% of the Chl *b* molecules in PSII are bound to LHCII (Jansson, 1994). Trimeric LHCII has been studied extensively by (sub)ps spectroscopy. It was shown that the major part of the Chl *b*–Chl *a* excitation energy transfer occurs with time constants ranging from $\sim$200 to $\sim$600 fs, and a small fraction occurs with a time constant of several ps (Bittner et al., 1994; Visser et al., 1996; Connelly et al., 1997b; Kleima et al., 1997). Subsequently, energy transfer occurs mainly between Chl *a* molecules, because their Q_y excited-state energy is much lower than that of Chl *b*. Due to spectral and spatial inhomogeneities, different transfer times coexist, and they range from hundreds of femtoseconds to many picoseconds for at least several pairwise transfer steps. In a (polarized) transient absorption study at room temperature by Kwa et al. (1992b), transfer times were observed ranging from $<$2 to 15–35 ps in trimeric LHCII. The latter time was tentatively assigned to transfer between monomers. A relatively slow process of 13 ps was also observed by Mullineaux et al. (1993) in an isotropic photon-counting study, although it was clear that faster processes should also be present. This was confirmed by Pålsson et al. (1994), who observed times of $\sim$2 and 10–20 ps. Savikhin et al. (1994) found transient absorption depolarization times ranging from 5 ps at room temperature to many tens of picoseconds at cryogenic temperatures, whereas Bittner et al. (1995) found an $\sim$14 ps spectral equilibration above 670 nm at 12 K. All these studies had in common that energy transfer was observed on a significantly longer time scale than 1 ps.

An extensive study of the Chl *a*–Chl *a* transfer kinetics in trimeric LHCII was performed by Visser et al. (1996, 1997) at 77 K. It was shown that excitation at 663 nm gave rise to an $\sim$2-ps transfer time, whereas excitation around 670 nm led to transfer steps of $\sim$400 fs and $\sim$15 ps. More recently, similar experiments were performed by Gradinaru et al. (1998) on monomeric LHCII at 77 K. In general, the results were comparable to those observed on trimers but more details were observed. Excitation at 663 nm showed a transfer time of 5 $\pm$ 1 ps toward longer wavelength pigments, and it was argued that this is due to the transfer originating from only one Chl *a* pigment. After excitation at 669 nm, two downhill transfer times of 300 fs and 12 ps were observed. Excitation toward longer wavelengths revealed that there is at least one other picosecond component present, whereas evidence was also found for additional subpicosecond equilibration events. Thus, it is clear that, within a monomeric subunit, both picosecond and subpicosecond processes occur. Recent 3PEPS measurements at room temperature led to the observation of Chl *a* equilibration times ranging from 300 fs to 6 ps (Agarwal et al., 2000). Most of the above-mentioned studies observed equilibration events within monomeric subunits (spectral equilibration) because no additional spectral equilibration is expected upon transfer between monomers, which are spectrally very similar. This was indeed confirmed by the study of monomeric LHCII by Gradinaru et al. (1998). The

results of the polarized studies possibly also reflect intermonomer transfer, but, without additional knowledge, it is impossible to draw quantitative conclusions about the exact amount.

Knowledge about the overall transfer process (spatial equilibration) in antenna systems can be obtained from singlet–singlet annihilation experiments (van Grondelle, 1985; Valkunas et al., 1999). The excited singlet (S) states of chromophores can act as mobile quenching centers for other S excitations in an aggregated/connected system. This leads to decreased excited-state lifetimes at high excitation intensities and concommitantly to a decrease of the fluorescence yield. By probing the intensity dependence of the excited-state lifetimes or the fluorescence quantum yield, which is proportional to the amplitude-weighted average lifetime, information can be obtained about the excitation mean hopping time between pigments, the excitation diffusion radius and fractal dimensions of the system (Den Hollander et al., 1983; Valkunas et al., 1995, 1999). For instance, the mean excitation transfer time between pairs of bacteriochlorophyll (BChl) pigment molecules was estimated to be equal to 0.5 ps in the simple LHA of the bacterium *Rhodospirillum rubrum* (so-called LH1 complexes), which contains only one pigment in one spectral form (den Hollander et al., 1983; Bakker et al., 1983; Valkunas et al., 1995). However, at lower temperatures (77 K), even this LHA demonstrates spectral inhomogeneity, which results in variation of the S–S annihilation efficiency for different excitation wavelengths (Deinum et al., 1989) and exhibits more complex annihilation kinetics than at room temperature (Valkunas et al., 1996). This is attributed to a fractal-like structural organization of the system at low temperature, resulting in a percolation type of energy transfer (Bunde and Havlin, 1991). Other LHA complexes both in bacteria and plants are spectrally more complex, containing several spectral forms of the same pigment molecules as well as different types of bacteriochlorophyll or chlorophyll molecules, and can be assembled in aggregates having different sizes of excitation migration domains. This spectral and structural diversity complicates the analysis of the annihilation processes.

Gillbro et al. (1988) studied S–S annihilation in aggregates of LHCII using picosecond pump-probe spectroscopy. From the lifetimes and corresponding amplitudes, a relative fluorescence quantum yield was calculated, which was determined as a function of excitation intensity. With the theoretical approach of Paillotin et al. (1979) and den Hollander et al. (1983), an average hopping time from Chl *a* molecules to their nearest neighbors was estimated between 1 and 5 ps. The uncertainty arises from the fact that the domain size cannot be determined, and, in fact, a distribution of sizes is present. Moreover, different lifetimes occur even in the absence of annihilation due to quenching centers in the aggregates (Ide et al., 1987; Mullineaux et al., 1993; Barzda et al., 1998). An upper limit for the average hopping time of 6 ps was estimated for aggregates of LHCII by Barzda et al. (1996) but heterogeneity of the preparations was not taken into account during the analysis.

Bittner et al. (1994) studied S–S annihilation in trimeric LHCII with the use of subpicosecond pump-probe spectroscopy. The observed annihilation could roughly be fitted with an exponential decay time of 28 ps. A slow annihilation rate of 0.25×10^{-9} cm^3s^{-1} was obtained, which was estimated using a model that in principle is only applicable to large aggregates. No attempt was made to estimate the average hopping time from this value. The rate of annihilation was smaller than values ($0.5–15 \times 10^{-9}$ cm^3s^{-1}) obtained with much longer pulses or for intact chloroplasts (Nordlund and Knox, 1981; Geacintov et al., 1977). This difference was attributed by Bittner et al. (1994) to differences in domain size, being smaller for LHCII trimers and larger for LHCII aggregates (Nordlund and Knox, 1981) and chloroplasts (Geacintov et al., 1977). In contrast to the results of Bittner et al., a study of the intensity dependence of the fluorescence yield and transmittance of trimeric LHCII complexes was described by assuming excitonically coupled pigments within the trimers, and, as a consequence, a very fast annihilation rate of the order of a few hundred fs was deduced in an indirect way (Schödel et al., 1996).

Here we present a study of S–S annihilation in LHCII in solutions with largely varying detergent concentrations to resolve apparent discrepancies in the literature about the rate of annihilation, to study the effect of aggregation on the annihilation in LHCII. Trimeric complexes are present in solution with high DM concentrations and the largest aggregates occur for low concentrations of detergent. In this way, important information is obtained about the spatial equilibration in LHCII, which complements the huge amount of data that has been collected on spectral equilibration. It allows us to estimate the contribution of the migration time through LHCII to the overall trapping process in PSII.

To circumvent the problem of the unknown size of the aggregates and the varying lifetimes that was met by Gillbro and coworkers (1988), we explicitly analyzed the kinetics of the annihilation in all cases, using the approach of Valkunas et al. (1999), that is based on the formulation by Suna (1970), instead of using the time-integrated signals. It is shown that the annihilation process in LHCII trimers is well described by a statistical approach, whereas the annihilation kinetics in aggregates is described by means of a kinetic approach with a time-dependent annihilation rate.

By applying these approaches, we are able to obtain the rate of annihilation normalized per trimer, which allows us to directly calculate the contribution of LHCII to τ_{mig} for the total trapping time in PSII. It is concluded that the outer antenna of PSII not only contributes to the trapping time via τ_{cs}, as was modeled by Roelofs et al. (1992), but also, to a significant extent, via the migration term (it contributes $\sim$160 ps).

MATERIALS AND METHODS

Stacked lamellar aggregates were isolated from dark-adapted two week-old pea (*Pisum sativum*) leaves according to the procedure described by Simidjiev et al. (1997). Isolation was performed in the dark. Isolated LHCII aggregates were stored at 4°C, and measurements were performed within two weeks after isolation. The critical micellar concentration (CMC) of the detergent in the LHCII samples, above which aggregates disassemble into trimers, was observed around 0.01% of *n*-dodecyl β-D-maltoside (DM) at 10 μg/ml Chl($a + b$) of LHCII (single photon timing measurements) and around 0.015% of DM at 30 μg/ml Chl($a + b$) of LHCII (absorption, fluorescence-intensity dependence, and transient absorption measurements). The CMC was determined from the characteristic increase of the fluorescence yield during titration of LHCII by the detergent (see Ide et al., 1987; Barzda et al., 1995; Simidjiev et al., 1997).

Fluorescence decay kinetics were measured by time-correlated single-photon counting using 593 nm, 8-ps excitation pulses from a synchronously pumped (frequency-doubled Nd:YAG laser, (Antares 76-S, Coherent, Palo Alto, California) cavity-dumped dye laser 700 dye laser with 7220 cavity dumper, dye: Rhodamin 6G) operated at a repetition rate of 148 kHz. Special care was taken to perform the measurements at low repetition rate and very low excitation intensity to avoid singlet-triplet and singlet-singlet annihilation, respectively. The excitation intensity at the sample was kept below 0.5 nJ/(pulse $*$ cm^2), which roughly corresponds to $2 * 10^{-6}$ excitation per one trimer of LHCII. Detection of the fluorescence was performed with a microchannel plate photomultiplier (R1564U-07, Hamamatsu, Japan) and a cut-off filter transmitting light above 680 nm was used to eliminate scattered excitation light. The response function of the apparatus (~80 ps FWHM) was obtained by detecting scattered excitation light from a turbid suspension. Fluorescence decays were deconvoluted using a sum of exponential terms with the apparatus response function.

Transient absorption investigations were carried out with a 2-ps time resolution pump-probe spectrometer, based on a home-made low-repetition rate passive-mode-locked Nd-glass laser (1 Hz repetition rate). The samples had an optical density of ~0.6 at the maximum of the red absorption band in a 5-mm cuvette. To obtain a homogeneous distribution of excitations throughout the sample, which is crucial in nonlinear experiments, the samples were excited at 527 nm (very low absorption) by the second harmonic of the basic laser radiation and probed at 680-nm wavelength that was selected from the white continuum generated in a water cell. The excitation beam diameter was ~1 mm and the diameter of the probe beam was ~0.3 mm, ensuring almost homogeneous excitation of the probed area. Pulse-to-pulse fluctuations of the excitation energy were less than 10%.

Measurements of the dependence of the fluorescence intensity on the excitation light intensity were performed using the second harmonic of Nd:$YAlO_3$ laser pulses at 534 nm with 10-ps duration at 5-Hz repetition rate. The time-integrated fluorescence intensity was measured by a photomultiplier at the maximum of the fluorescence band around 680 nm. Calibrated filters were used to attenuate the fluorescence at high excitation intensities. The edges of the pump beam were cut off at 70% of the maximal intensity by a diaphragm that was placed in front of the sample.

MODELING OF THE S–S ANNIHILATION

The S–S annihilation theory is well developed for spectrally homogeneous molecular systems (see, for instance, van Amerongen et al., 2000). When comparing the size of an aggregate with the excitation-diffusion length, two limiting cases can be distinguished, namely those of large and small aggregates (van Grondelle, 1985; Valkunas et al., 1995, 1999). For small aggregates, which are much smaller than the actual excitation-diffusion length, the aggregate can be viewed as a supermolecule being characterized mainly by energy levels reflecting single and multiple excitations, and the statistical approach can be used in this case (Paillotin et al., 1979; Nordlund and Knox, 1981; den Hollander et al., 1983; van Grondelle, 1985). According to this approach the initial distribution of excitations in the ensemble of aggregates mainly determines the annihilation process, which can be viewed as a sequential relaxation process in a multiexcitation level scheme, described by the Master equation,

$$\frac{\partial}{\partial t}p_i(m,t) = -\left[\frac{i}{\tau} + \frac{\gamma}{2}i(i-1)\right]p_i(m,t) + \left[\frac{i+1}{\tau} + \frac{\gamma}{2}i(i+1)\right]p_{i+1}(m,t), \quad (2)$$

where $p_i(m, t)$ is the probability that at time t there are i excitations present, given m excitations at $t = 0$ ($p_i(m, 0) = \delta_{m,i}$), τ is the linear excitation decay time, and γ is the S–S annihilation rate. The average number of excitations remaining in the aggregate at time t is given by

$$\langle i\rangle_m = \sum_{i=1}^{m} i p_i(m,t). \quad (3)$$

When the above summation is applied to each term in Eq. 2 we obtain the equation,

$$\frac{d\langle i\rangle_m}{dt} = -\frac{\langle i\rangle_m}{\tau} - \frac{\gamma}{2}\langle i(i-1)\rangle_m. \quad (4)$$

If the initial distribution of excitations in the complexes/aggregates obeys a Poisson distribution, then $\langle i(i-1)\rangle = \langle i\rangle^2$, and Eq. 4 is analogous to the kinetic equation used for extended aggregates (see below). However, as time progresses, the probabilities $p_i(m, t)$ will differ from those given by the initial Poisson distribution. Moreover, the initial distribution in time is mainly determined by the shape of the excitation pulse, which can be taken into account by adding the corresponding generation function $\sigma J(t)(i-1)p_{i-1}(m, t)$ to Eq. 2, where $J(t)$ is the intensity of the excitation pulse and σ is the absorption cross section. To obtain the correct temporal evolution Eq. 2 has to be solved numerically.

For extended aggregates (i.e., when the actual size of the domain is comparable to or larger than the excitation diffusion length) a kinetic description of the excitation evolution can be used. Such an approach was originally formulated by Suna (1970) for molecular crystals and later developed for studies of excitation kinetics in large molecular aggregates (Valkunas et al., 1995, 1999). It is represented by the equation,

$$\frac{dn}{dt} = \sigma J(t)\left[N - \left(1 + \frac{\sigma_{em}}{\sigma}\right)n\right] - \frac{n}{\tau} - \frac{\gamma(t)}{2}n^2, \quad (5)$$

where N is the number of pigment molecules per aggregate (or that part of the aggregate that is used for normalization) absorbing at the excitation wavelength, n is the total number of excited molecules in the aggregate, σ is the molecular absorption cross section at the excitation wavelength, σ_{em} is the molecular cross section for the corresponding stimulated emission, $J(t)$ is the excitation pulse intensity, τ is the linear excitation decay time, and $\gamma(t)$ is the rate of S–S annihilation. For comparing annihilation in trimers and various aggregates, we normalize the values n, σ, and N per trimer. In this way, the value of $\gamma(t)$ will also be normalized per trimer. Note, however, that, in doing so, it is neglected that $f_d(N)$ is different (see Introduction). In fact, this factor will be larger for large aggregates although the variation is not very pronounced (see also Discussion). After the excitation pulse, the solution of Eq. 5 can be described by the formal equation,

$$n(t) = \frac{n_0\exp(-t/\tau)}{1 + (n_0/2)\int_0^t \gamma(t')\exp(-t'/\tau)\,dt'}, \quad (6)$$

where n_0 is the initial population created by the excitation pulse.

The time dependence of $\gamma(t)$ is determined by the pair correlation function of the excitations (Suna, 1970; Valkunas et al., 1995, 1996, 1999). For a diffusion-limited process like the annihilation in extended systems, the time dependence of $\gamma(t)$ can be approximated by a power law (Bunde and Havlin, 1991), i.e.,

$$\gamma(t) = \frac{\gamma_0}{t^{\alpha}}, \tag{7}$$

where α is determined by the geometrical characteristics of the exciton diffusion in the aggregate. The parameter γ_0 has the dimensions of $\mathrm{ps}^{\alpha-1}$. In regular and homogeneous Euclidean structures, α is related to the structural dimension d_s as (Bunde and Havlin, 1991)

$$\begin{aligned} \alpha &= 1 - \frac{d_s}{2} \quad \text{if} \quad d_s \le 2, \\ \alpha &= 0 \qquad\quad \text{if} \quad d_s \ge 2. \end{aligned} \tag{8}$$

In case of spatial irregularities or spectroscopic heterogeneity, d_s can be considered as a fractal (spectral) dimension (Bunde and Havlin, 1991). It is worth noting that the excited-state decay kinetics can provide direct information about the fractality of the structure/spectroscopic organization of the system under consideration (Valkunas et al., 1996), which cannot be directly obtained from the time-integrated characteristics, such as, e.g., the dependence of the fluorescence quantum yield on the excitation intensity.

Thus, substituting Eq. 7 into Eq. 6 for the short-time kinetics ($t < \tau$), we obtain the analytical solution

$$n(t) = \frac{(1-\alpha)n_0}{1 - \alpha + (n_0/2)\gamma_0 t^{1-\alpha}}, \tag{9}$$

which, for $\alpha = 0$ reduces to

$$n(t) = \frac{n_0}{1 + (n_0/2)\gamma_0 t}. \tag{10}$$

Eq. 9 can be rewritten as

$$\frac{1}{n(t)} - \frac{1}{n_0} = \frac{\gamma_0/2}{1-\alpha} t^{1-\alpha} \tag{11}$$

and in a log-log representation, this gives

$$\log\left(\frac{1}{n(t)} - \frac{1}{n_0}\right) = \log\left(\frac{\gamma_0/2}{1-\alpha}\right) + (1-\alpha)\log t. \tag{12}$$

According to Eqs. 11 or 12, a graph of the time dependence of the function $1/n(t) - 1/n_0$ gives information about the time-dependence of the annihilation rate, as is demonstrated in Fig. 1. The normalization of the excitation population (and thus, also of the annihilation rates) per trimer for the large aggregates is convenient for a comparison of both the kinetic and statistical approach. The obtained annihilation rate after this normalization is similar for both methods. Both approaches are visualized in Fig. 1. Qualitatively, the curve obtained with the statistical approach is similar to the one obtained by the kinetic approach with a time-dependent annihilation rate giving a downward deviation in both cases. For the statistical description, this is a consequence of the finite population of excitations in a trimer, leading to a strong deviation from the linear behavior toward the situation corresponding to $(\gamma/2)i(i-1) = 0$ for $i = 1$. Both methods (kinetic approach according to Eq. 5 and statistical approach according to Eq. 2) will be used for describing the S–S annihilation in trimers and aggregates.

The dependence of the fluorescence yield on the excitation intensity can also be calculated for both methods. (For details of such calculations see Paillotin et al., 1979; van Grondelle, 1985 and Valkunas et al., 1999.) In the case of the statistical approach and for fast annihilation, i.e., assuming that

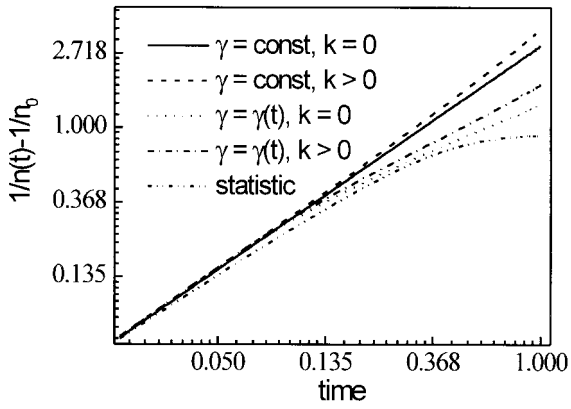

FIGURE 1 Time dependence of $1/n - 1/n_0$ calculated for various models. Relative units are used. The annihilation rate was calculated according to a modified version of Eq. 7, i.e., by assuming that $\gamma = \gamma_0[\tau_\gamma/t]^{\alpha}$, and the parameters in relative units used for the calculations are as follows: $\gamma_0 = 3$, $\alpha = 0.5$, $\tau_\gamma = 1/15$, $k = 1/\tau = 0.4$. The solid line corresponds to the situation of $\gamma = \gamma_0 =$ constant and $k = 0$, the dashed line to $\gamma = \gamma_0 =$ constant and $k \neq 0$, the dotted line to $\gamma = \gamma(t)$ and $k = 0$, the dashed-dotted line to $\gamma = \gamma(t)$ and $k \neq 0$, the dashed-double dotted line reflects the statistical approach with $\gamma = \gamma_0$ and $k = 0$.

$\gamma\tau \gg 1$, it follows from Eqs. 2 and 3 that the fluorescence (F) intensity plotted as a function of laser intensity will saturate in an exponential way:

$$F = \Phi_0(1 - e^{-\sigma J}), \tag{13}$$

where $J = \int J(t)\,\mathrm{d}t$ and Φ_0 is the fluorescence quantum yield under annihilation-free conditions. For extended aggregates, when the annihilation rate is assumed to be time-independent, integration of Eq. 6 leads to

$$F = \frac{2\Phi_0}{\gamma_0\tau} \ln\left(1 + \frac{\gamma_0\tau\sigma J}{2}\right). \tag{14}$$

It is possible to link the rate of annihilation to τ_{mig}, as discussed in the Introduction (Eq. 1). There is no fundamental difference between the formal description of the trapping process as given in the Introduction and the S–S annihilation presented in this section (den Hollander et al., 1983). In the former case, the RC acts as an immobilized trap, whereas, in the latter case, one excited molecule acts as a mobile trap for the other. However, in the case of S–S annihilation, the trap moves with the same speed as the excitation and therefore annihilation occurs approximately twice as fast as trapping by an RC. We compare both processes in slightly more detail. The trapping process as described in the Introduction is given for a regular lattice, and, in the case of annihilation, this would mean that $\alpha = 0$ or that the annihilation rate is time independent. The term τ_{trap} was given to be equal to $N\tau_{cs}$ for a regular lattice, and, in the case of annihilation, we would have to replace τ_{cs} by τ_{vib}, which reflects the vibrational relaxation after an excitation of one pigment has been accepted by the other excited molecule and the vibrational relaxation leads to the loss of one excitation. Such a relaxation process typically occurs on a time scale of hundreds of femtoseconds. The term τ_{del} would not be necessary for annihilation if energy transfer from an excited molecule to an unexcited molecule would be equally fast as to an excited molecule (which would then be responsible for annihilation). This is only approximately true because the excited-state absorption is somewhat smaller than the ground-state absorption in the wavelength region of interest (Becker et al., 1991). This leads to a decreased Förster overlap function and thus to a decreased transfer rate. Below, we neglect this difference. This leads to a slight overestimation of the last term τ_{mig} which is apart from a factor of 2

identical for the case of trapping by the reaction center and that of S–S annihilation (see above), the latter process being faster.

RESULTS

The LHCII absorption spectrum is almost independent of the degree of aggregation (Fig. 2), which was varied by changing the concentration of detergent in the sample (Barzda et al., 1994). In contrast, the fluorescence yield and kinetics depend significantly on the degree of aggregation. Upon nonselective excitation of Chls at 593 nm with low-intensity picosecond laser pulses, when both S–S and S–T annihilations are excluded, the fluorescence-relaxation kinetics is faster for larger aggregates (Fig. 3, see also Ide et al., 1987; Mullineaux et al., 1993; Vasil'ev et al., 1997). This may be due to the creation of quenchers upon aggregation or to the fact that quenchers that were present in a small fraction of the trimers can also quench excitations in other trimers, due to inter-trimer transfer in the aggregates. The fluorescence decay kinetics is exponential for trimers, and, for larger aggregates, it may well be approximated by two exponentials, whereas the relative amplitudes and decay times depend on the degree of aggregation (see Table 1). As shown in Table 1, both lifetimes increase upon increasing the detergent concentration and thus diminishing the average size of the aggregates. A limited number of quenching centers is probably present in aggregates. When the average size of the aggregates is reduced by adding the detergent (Ide et al., 1987; Barzda et al., 1994, 1995), the number of quenching centers per aggregate also decreases and the relative number of (small) aggregates without quenching centers increases. It is important to note that the presence of different kinetic components can impair the interpretation of annihilation experiments in which fluorescence yields are measured as a function of excitation intensity. Thus, the changes in the relative amplitudes resemble the changes in the amount of aggregates with and without quenchers.

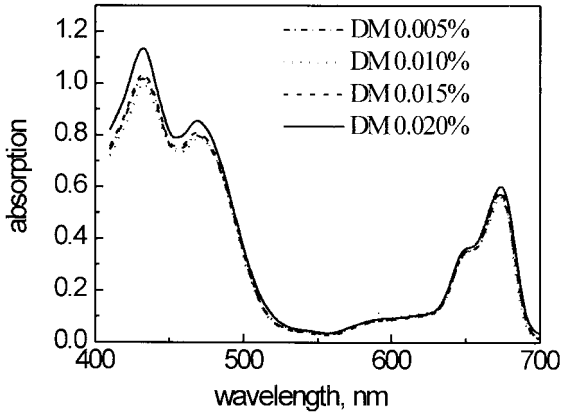

FIGURE 2 The absorption spectra of LHCII at different DM concentrations. The concentration of LHCII was 30 μg/ml of Chl(a + b).

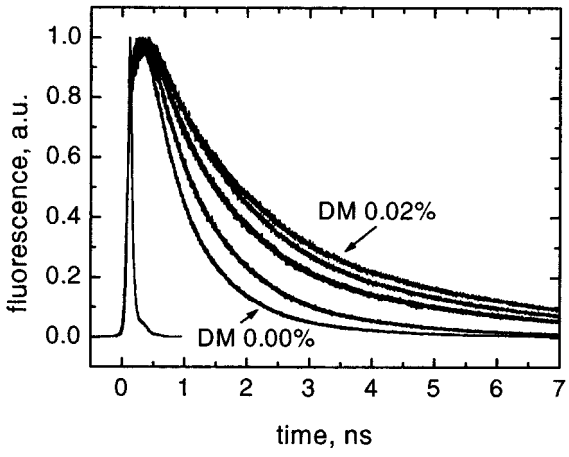

FIGURE 3 The normalized fluorescence kinetics of LHCII at different DM concentrations. The response function is also shown. Kinetic curves correspond to a DM concentrations of 0, 0.005, 0.010, 0.015, and 0.02%, being fastest for 0% DM and gradually becoming slower with the increase of DM concentration. The concentration of LHCII was 10 μg/ml of Chl(a + b). Fitting parameters are presented in Table 1.

Around the CMC, a transition from LHCII aggregates to trimers takes place and all the quenching centers disappear. This results in a monoexponential fluorescence decay, and the lifetime of about 3.4 ns is characteristic for unquenched Chls in protein.

The dependence of the integrated fluorescence on the excitation intensity is shown in Fig. 4. An approximately linear dependence is observed for all samples at low excitation conditions, whereas, at higher excitation intensities, a deviation from linearity, caused by S–S annihilation, is observed. For trimers, the intensity threshold for S–S annihilation should correspond to conditions where, on the average, more than one excitation per trimer is generated by a single pulse. Similarly, the S–S annihilation in larger aggregates should start at excitation intensities where, on the average, more than one excitation is created in the aggregate or in a part of the aggregate (for large aggregates), restricted by the excitation-diffusion radius.

More quantitative conclusions concerning the rate of energy transfer and the size of the domain determined by the excitation-diffusion length in the aggregate can be obtained from the excitation-decay kinetics under S–S annihilation

TABLE 1 Parameters of two exponential fit of fluorescence kinetics of the LHCII

DM (%)	A_1	τ_1 (ps)	A_2	τ_2 (ps)
0.000	0.88	713	0.12	1775
0.005	0.57	890	0.43	1614
0.010	0.42	1347	0.58	3601
0.015			1.00	3220
0.020			1.00	3491

The concentration of LHCII was 10 μg/ml of Chl(a+b).

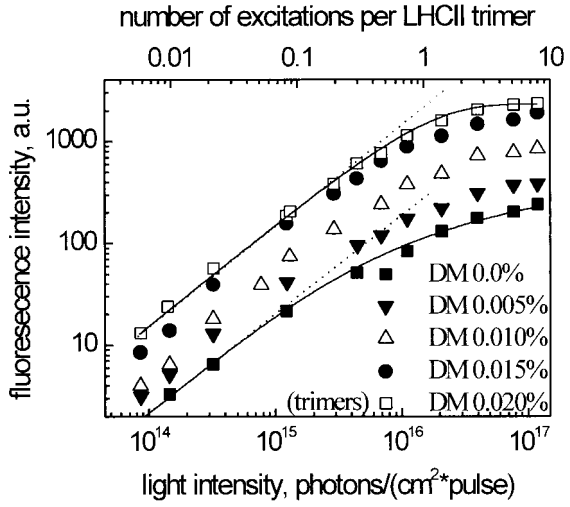

FIGURE 4 The dependence of the integrated fluorescence of LHCII on the excitation intensity at different DM concentrations. Solid curves are calculated according to the statistical approach (for trimers) and the kinetic approach (for large aggregates). Dotted lines reflect a linear dependence. The top axis is related to the theoretical curves. The value of the fluorescence quantum yield is used as a fitting parameter, to fit the experimental curves at low excitation intensities.

conditions. The results of transient absorption kinetics at 680 nm performed with ~2-ps pump laser pulses are shown in Fig. 5 for different detergent concentrations, which result in different sizes of the aggregates. The right vertical axis indicates the relative amount of excited pigments evaluated according to the relation

$$n = \frac{\Delta A}{A} \cdot \frac{\sigma_{\text{abs}}}{\sigma_{\text{abs}} + \sigma_{\text{em}}}, \tag{15}$$

where A is the absorbance of the sample, ΔA is the difference absorbance, σ_{abs} and σ_{em} are the absorption and stimulated emission cross sections, all at the same probe wavelength (680 nm). The latter value was estimated from the fluorescence spectrum according to the procedure described by Becker et al. (1991).

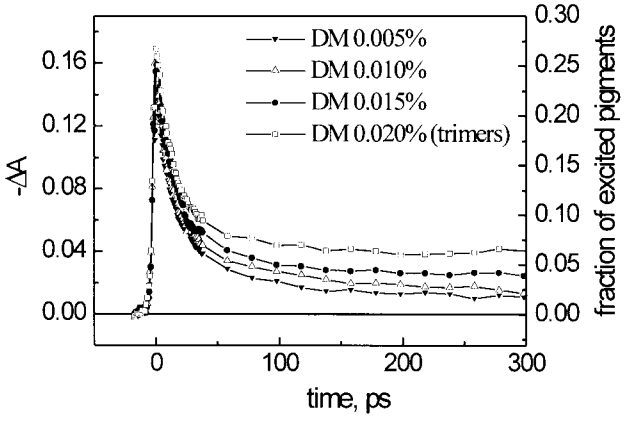

FIGURE 5 The bleaching kinetics at 680 nm at different DM concentrations. The concentration of LHCII was 30 μg/ml of Chl(a + b).

The decay curves shown in Fig. 5 are not mono-exponential. The fast part of the decay proceeds during the initial 30–50 ps, and afterward, the decay kinetics slows down. This slow part of the kinetics is dependent on the degree of aggregation and is faster for larger aggregates. The relative amplitudes of the fast and slow components also vary for different detergent concentrations.

DISCUSSION

Annihilation in trimers

The amount of fluorescence as a function of the excitation intensity is shown for trimeric LHCII in Fig. 4. Whereas the kinetic approach (Eq. 14) fails, the statistical approach (Eq. 13) can nicely explain the intensity dependence. Assuming that Poisson statistics determines the probability of generating a certain number of excitations in a trimer and in case of fast annihilation (compared to the excitation lifetime) the deviation from linearity on a log-scale corresponds to 1/e at the intensity of 1 excitation (on average) per domain (see Eq. 13). The deviation appears roughly at $1.5 * 10^{16}$ photons $*$ cm^{-2}. Estimation of the excitation density with $\sigma = 2 * 10^{-16}$ cm^2 at the excitation wavelength (534 nm) leads to approximately 2 excitations per trimer instead of one. Given the uncertainty in the light intensity in the overlap region of pump and probe beam and the uncertainty in the absorption cross section at 534 nm (the absorption is very low in this region), the intensity dependence is close to what one would expect for individual trimers, and it is essentially different from what one would expect for aggregates.

In Fig. 6 *a*, annihilation on a picosecond time scale is shown for trimeric LHCII together with the best fit using the statistical approach, and the obtained annihilation rate is $\gamma^{-1} = 24$ ps. The fitting parameters are as follows: τ_{pulse}, reflecting the apparatus function, is well described by a Gaussian function of 4-ps width (FWHM), whereas the linear relaxation time was taken to be $\tau = 3$ ns (close to the value determined from the annihilation free fluorescence kinetics, see Table 1; the accuracy is more than sufficient for the description of the short-time kinetics). Based on the changes in optical density (see Fig. 5), the number of excitations was estimated to be $J = 5$ photons/trimer. We also tried to describe the trace for the trimers with the kinetic approach but this turned out to be impossible. In the figure, it is shown that, to correctly fit the first 30 ps where most of the annihilation takes place, we need annihilation parameters that lead to a large overestimation of the amount of annihilation at longer times. The explanation is obvious, after ~50 ps all annihilation is over in the trimers that are relatively small in size, whereas the kinetic approach is suited for large systems where the annihilation process

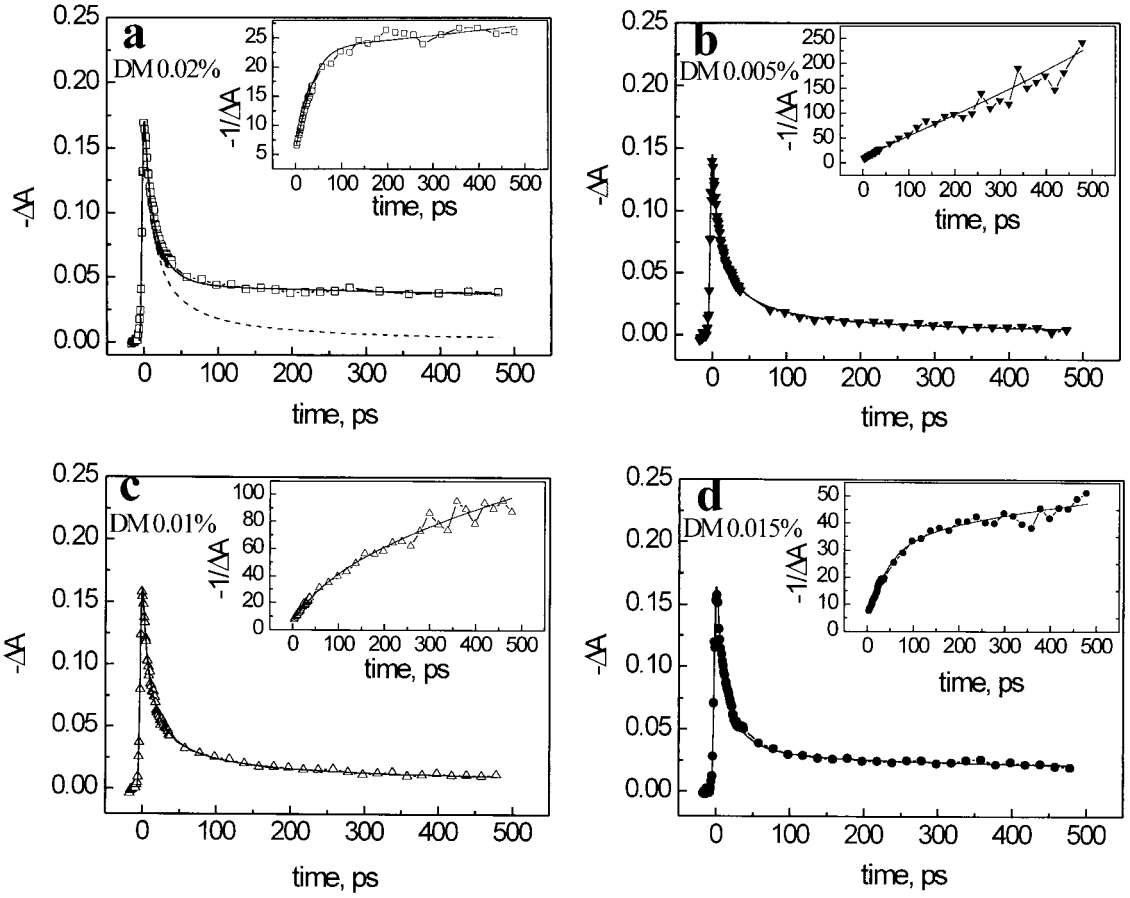

FIGURE 6 The annihilation kinetics for LHCII at a DM concentration of (*a*), 0.02%; (*b*), 0.005%; (*c*), 0.01%; and (*d*), 0.015%. *Solid lines*, theoretical fitting of the experimental data (parameters are presented in Table 2). The dashed line in (*a*) shows fitting according to the kinetic approach. The inserts show the same data presented on a reversed scale.

continues during the entire excited-state lifetime. It should be noted that the annihilation mainly takes place between excitations on Chl *a* molecules. The laser light at 527 and 534 nm excites both carotenoids and chlorophylls but nearly all excitations are transferred to Chl *a* within 1 ps (Peterman et al., 1997; Connelly et al., 1997a), which is just below the time resolution of our experiments. The findings will be discussed in more detail below.

Annihilation in LHCII aggregates

It is well known that lowering the detergent concentration below the CMC leads to aggregation of LHCII (Burke et al., 1978; Ide et al., 1987; Barzda et al., 1994). Aggregates of various sizes occur but also different excited state lifetimes are present for these aggregates and the average lifetime goes down compared to that of trimers (Ide et al., 1987; Mullineaux et al., 1993; Vasil'ev et al., 1997). Both the unknown sizes and the different lifetimes led to complications for the interpretation of the annihilation results of Gillbro et al. (1988). The average lifetime shortens to below one ns (under annihilation free conditions) as can be seen in Table 1. The amount of fluorescence as a function of the excitation intensity for the aggregates in the absence of detergent is shown in Fig. 4. The shape of the curve is clearly different from that for trimers. In this case, the intensity dependence cannot be described by Eq. 13 (statistical approach) but it is nicely fitted with Eq. 14 (kinetic approach). The deviation from linearity on a log–log-scale now appears at significantly lower excitation intensities. Also taking into account that the average excited-state lifetime (in the absence of annihilation) is several times shorter than for trimers, it is clear that excitations can "travel" through many trimers before they annihilate.

In Fig. 6 *b* the time-resolved annihilation of aggregated LHCII in 0.005% DM is given. It should be noted that the LHCII concentration in these measurements was three times as high as in the fluorescence experiments, presumably leading to larger aggregates, but, in contrast, a higher detergent concentration was taken, leading to a decrease of aggregate size. Despite these two counteracting conditions, the aggregates in the pump-probe and fluorescence experi-

ments are most likely slightly different. An almost perfect description of the time-dependence of the transient absorption over many hundreds of picoseconds is obtained with the kinetic approach using $\gamma_0^{-1} = 16$ ps and $\alpha = 0.1$. From Fig. 5, it was already clear that annihilation in aggregates continues for many hundreds of picoseconds, indicating efficient energy transfer. However, the fit in Fig. 6 *b* shows that, with only one (time-dependent) rate, the time dependence can be described over a large time window, covering both transfer within a trimer and transfer between many trimers. This demonstrates that a lamellar LHCII aggregate should be considered as a continuous lattice and not as a collection of trimers where energy transfer within trimers occurs on a different time scale than transfer between trimers. For regular 2- and 3-dimensional lattices, one does not expect any time dependence of the annihilation rate, whereas, for 1-dimensional lattices, a strong time dependence is expected. The small value of α indicates that there is only a limited time dependence, so that the aggregates can approximately be considered as regular 2- or 3-dimensional lattices (which is useful for further interpretation, see below), the deviation being due to structural and spectral inhomogeneity.

Comparison of the annihilation LHCII in different detergent concentrations

In the previous sections, the differences of the annihilation in trimers and large aggregates in high and low detergent concentrations, respectively, were discussed. At intermediate detergent concentrations also "intermediate behavior" is observed as is clear from Fig. 5. The experimental data are shown in a $1/n(t) - 1/n_0$ representation in Fig. 7. We observe an initial linear regime for all degrees of aggregation, whereas, at the threshold time $t_c \approx 30$ ps, this temporal dependence starts to deviate for trimers. For large aggregates, this deviation sets in at later times (well over $t_c \approx 30$ ps). For the different states of aggregation, the curves are slightly shifted along the ordinate axis. Note that, within the experimental errors, there is no change in the initial slope upon aggregation, and because the value of the slope is close to unity it points out that α is small, i.e., the time dependence of the annihilation rate in aggregates is weak. Significant differences occur at longer times where the slope starts to change, becoming smallest for trimers. This result is understandable: the threshold time t_c corresponds to the annihilation time γ^{-1} in the trimer, whereas at later times, the slope is almost parallel to the time axis because $\sim$1 excitation per trimer is left and the annihilation is switched off. The slight upward shift at early times for large aggregates as compared to trimers must be attributed to $\log(\gamma_0/2(1-\alpha))$ according to Eq. 12, indicating a 1.5 times increase in the mean rate of annihilation, in agreement with the results given above (note that α is small).

Because, at intermediate DM concentrations, the curves fall between those of aggregates and trimers, one might, in first approximation, assume that the samples contain a mixture of large and small aggregates which could, to some extent, also explain the aggregation-dependent linear fluorescence decays (see Fig. 3, Table 1), where the amplitudes of the exponential components might be attributed to relative amounts of LHCII in large and small aggregates. The S–S annihilation kinetics of LHCII at intermediate DM concentration could indeed be fitted with the assumption of the coexistence of small domains and large domains for which the statistical and the kinetic description hold, respectively. The fitting results are shown in Fig. 6, *c* and *d*. The corresponding fitting parameters and the ratio of the amplitudes are presented in Table 2. One might try to estimate the relative amounts of trimers in small and large aggregates at a particular DM concentration from the fitted amplitudes. Values of the relative amplitudes and the relaxation times obtained from the best fit (see Table 2) are slightly different from those obtained from fitting the fluorescence kinetics under low excitation intensity conditions (Table 1). Different LHCII concentrations were used in annihilation and linear fluorescence lifetime measurements. The higher LHCII concentration slightly shifts the CMC to a higher

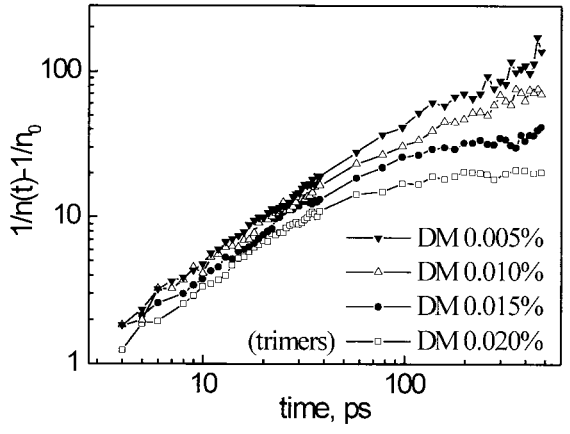

FIGURE 7 Experimental bleaching kinetics of LHCII at 680 nm at different DM concentrations presented as the time dependence of $1/n - 1/n_0$.

TABLE 2 Fitting parameters of the annihilation kinetics in LHCII aggregates at different DM concentrations (see Fig. 6)

	Aggregate S–S annihilation rate normalized to the trimer $\gamma_0^{-1} = 16$ ps			Trimer S–S annihilation rate $\gamma^{-1} = 24$ ps	
DM (%)	A_1	τ_1 (ps)	α	A_2	τ_2 (ps)
0.005	1.00	900	0.2		
0.010	0.85	1350	0.2	0.15	3000
0.015	0.48	2500	0.1	0.52	3000
0.020				1.00	3000

The concentration of LHCII was 30 μg/ml of Chl(a+b).

detergent concentration because more protein binds more detergent (Ide et al., 1987). Comparison of the annihilation kinetics and the linear fluorescence decays can be done by lowering the concentration of DM by approximately 0.005% for annihilation measurements. This reveals good agreement between both data sets. Although the above approximation seems to give consistent results, we hasten to say that the analysis and interpretation should not be taken too literally. The main point is that, at intermediate DM concentrations, the kinetics can be understood in terms of mixtures of small and large aggregates and that only at very low detergent concentrations one can describe the kinetic behavior with the kinetic model.

The relation between the annihilation rate in LHCII trimers and aggregates

The inverse annihilation rate γ^{-1} for trimers is 24 ps, whereas $\gamma_0^{-1} = 16$ ps for aggregates after normalization to trimers. Both rates are not exactly the same, which is partly due to the different theoretical descriptions. However, they are of a similar order of magnitude. A decrease of the inverse rate is not expected for regular lattices that increase in size, because $f_d(N)$ increases and the opposite effect might have been anticipated. The most straightforward explanation is that some Chls that are relatively far away from the bulk of the pigments in individual trimers, get in better contact with the bulk of Chls in aggregates, for instance, through short distances with respect to Chls on neighboring trimers. New routes for energy transfer and annihilation are thus opened, and, effectively, this means that τ_{del} decreases for aggregates. Below we will use the obtained rate for aggregates to estimate τ_{mig} in PSII. Evidently, its contribution to the total trapping time will increase, if the obtained annihilation rate for trimers is used.

The contribution of LHCII to the overall trapping time in PSII

It is possible to estimate the contribution of LHCII to τ_{mig} in a direct way from the obtained results, without estimating the hopping rate as was already indicated in the Theory section. Per RC, there are approximately four trimers (Jansson et al., 1997). Thus, each trimer adds 2×16 ps to the total migration time τ_{mig}. Therefore, four LHCII trimers per RC add 128 ps to the total excited state lifetime, assuming that intra- and intertrimer energy transfer is similar in lamellar aggregates and PSII. Intertrimer transfer in aggregates appears to be not a rate-limiting event (see above). If it is slower in PSII, the total contribution of τ_{mig} will increase. In contrast, if it is faster in PSII, not much will change, because intratrimer transfer (which is also relatively slow) will become rate limiting; the assumption is made that intratrimer transfer is similar in PSII and LHCII aggregates. In fact, reported annihilation rate constant in PSII membranes is only slightly slower than our obtained value for LHCII (Wulf and Trissl, 1996). The outer antenna of PSII contains, in addition to LHCII, also CP24, CP26, and CP29, which are presumably rather similar to monomeric LHCII with respect to structure and content of Chl *a* molecules (Bassi et al., 1997). Therefore, on average, the total contribution of the outer antenna to τ_{mig} is estimated to be ~160 ps, which is rather close to the value of 290 ps observed for PSII (see above). This implies that excitation trapping in PSII cannot be trap limited. It should be noted that, due to heterogeneity, the number of LHCII trimers per RC might strongly vary throughout the thylakoid membrane, but the important point is that each trimer of LHCII adds ~32 ps to the total migration time for the RC to which it is connected.

As already mentioned, numerous studies have been performed to elucidate the dynamics of light-harvesting and charge separation in PSII, with many different results. Roelofs et al. (1992) collected an extensive data set for intact pea chloroplasts and global lifetime analyses indicated PSII lifetimes of 290 and 630 ps for open RCs. The data were interpreted in terms of heterogeneity of PSII and the kinetics were explained with the exciton-radical pair equilibrium model. In view of the results of Boekema et al. (1999a,b) (see Introduction), heterogeneity in the organization is certainly an important factor. Our results do not support a diffusion-limited model (contribution of 160 ps of the outer antenna to τ_{mig} is too small) but they indicate that the contribution of τ_{mig} to τ_{exc} (Eq. 1) cannot be neglected, and it will vary for different organizations of LHCII. It is important to note that both transfer between LHCII trimers and "back" transfer from the core to LHCII are likely to occur in view of the structural organization and the small differences in excited state energy (see Introduction).

Comparison of energy transfer between Chl *a* molecules in LHCII and PSI

It is of interest to compare transfer between Chl *a* molecules in PSI and LHCII (forming a significant part of PSII). Excitation of Chl *a* in PSI of *Synechocystis* sp. PCC 6803, which contains approximately 100 Chls *a*, leads to trapping with a time constant of 23–24 ps (Savikhin et al., 1999; Gobets et al., 1998). This is even faster than the spatial equilibration time of 32 ps for a single LHCII trimer, which contains only 21 Chl *a* molecules. In addition, the trapping time in PSI is probably, to a large extent, contributed to by relative slow transfer from the antenna pigments to the primary donor (Gobets et al., 1998 and references therein). This means that energy transfer between Chl *a* molecules in LHCII occurs on a time scale that is an order of magnitude larger than in PSI. A qualitative explanation for this difference is the fact that the Chl *a* pigment density per unit of area is approximately a factor of two lower in LHCII as compared to PSI (Kühlbrandt et al., 1994; Krauss et al.,

1996). Given the strong dependence of the energy transfer rate on the distance r between donor and acceptor molecules (r^{-6}), this can, to a large extent, account for the observed differences. The fact that the overall trapping time for PSI is so much faster than for PSII, must be partly because the excited state of P700, the primary donor in PSI, is significantly lower in energy than that of P680, the primary donor in PSII, reducing the rate of back transfer of excitation energy from primary donor to the antenna.

APPENDIX: COMPARISON WITH PREVIOUS ANNIHILATION STUDIES ON LHCII

In this Appendix, we show that the annihilation results obtained in this study are in agreement with previous annihilation studies, in which either regular lattice models were assumed or the presence of heterogeneity in the preparations was neglected in most cases. Note that the present study explicitly accounts for spectral/structural inhomogeneity and variation in the degree of aggregation and makes explicit use of the annihilation behavior as a function of time. From the results obtained for aggregates, the energy-transfer rate between Chl *a* molecules can be estimated if a regular lattice is assumed. To do so, we neglect the (weak) time dependence of the annihilation rate. For rough estimations, the following equation, which is, strictly speaking, only correct for an infinitely large system of connected trimers (Valkunas et al., 1999), can be applied:

$$\gamma_0 = \frac{4\pi DR}{V}, \tag{16}$$

where D is the excitation diffusion constant, V is the volume of the aggregate (domain), R is the reaction radius of the annihilation process (meaning that two excitations inevitably annihilate immediately when they are at a distance smaller than this radius). In the nearest-neighbor approximation $D = a^2/\tau_{hop}$ where a is the interpigment mean distance, and τ_{hop} is the mean excitation hopping time between pigments. We use the following estimates for the remaining parameters: $R = a$ (assuming that the S–S annihilation is a migration-limited process as discussed above [see also Valkunas et al., 1995, 1999]), $V = \frac{4}{3}\pi Na^3$, where N is the number of pigments in the aggregate. By using the normalization of the values per trimer, i.e., by taking into account 21 Chl *a* molecules and $\gamma_0^{-1} = 16$ ps, it follows that $\tau_{hop} = 2.3$ ps.

An alternative way for obtaining an estimate for τ_{hop} runs as follows: As discussed in the Introduction, we use $2\gamma_0^{-1} = 0.5Nf_d(N)\tau_{hop}$. The annihilation rate is normalized per trimer, which suggests that we need to take a value of $N = 21$ (number of Chl *a* molecules per trimer) to determine the value of $f_d(N)$, but the rate was actually determined for large aggregates for which the number of pigments is much larger and then it was normalized to trimers. Therefore, its value would be approximately 0.8 for a square lattice and 0.6 for a hexagonal lattice (Kudzmauskas et al., 1983). Here, we simply take a value of 0.7. This leads to $\tau_{hop} = 4.2$ ps. Therefore, it is clear that the exact value depends on the model that is applied and the organization of the lattice that is assumed. However, it is also evident that whatever model is taken, an average hopping time of several picoseconds is found. Note, however, that the meaning of an average hopping time is very limited, given the large variation in individual transfer rates. However, it allows a comparison with previous studies that were analyzed in terms of average hopping rates.

An early annihilation kinetics study of LHCII was performed by Gillbro et al. (1988). Because the preparation contained a mixture of different domain sizes and an estimate was made for the average domain size, only a rough estimate could be given for the average hopping rate, and it was proposed that it would probably lie between $(1\text{ ps})^{-1}$ and $(5\text{ ps})^{-1}$. The estimates are in rather good agreement with the current findings. The obtained value for the average hopping time is smaller than the value of 6 ps that was obtained as an upper limit in recent S–S annihilation experiments where the excited dynamics on a picosecond time scale was also studied, but the heterogeneity of the samples was not taken into account (Barzda et al., 1996). Concomitantly, a lower value of α was found in that study. Our results on trimeric LHCII are qualitatively similar to those obtained by ultrafast measurements by Bittner et al. (1994). The quantitative differences (compare 28 ps [Bittner et al., 1994] and 24 ps in our case for the annihilation rates in trimers) are mainly related to the different approaches for describing the S–S annihilation process (exponential approximation in Bittner et al., 1994). The annihilation in LHCII was also addressed in a steady-state fluorescence yield and transmittance by Schödel et al. (1996). Based on their own results, these authors explained the intensity dependence of the transient absorption kinetics as presented by Bittner et al. (1994). However, Schödel et al. used a coherent exciton picture and determined, in an indirect way, the rate of annihilation. It turned out to be 50 times faster than the annihilation measured by Bittner et al. Our measurements clearly support the findings of Bittner et al. and are in disagreement with the interpretation by Schödel et al., thereby showing that the coherent approach is not applicable in this case.

The authors thank Dr. J. P. Dekker for helpful discussions.

V.B. was supported by European Molecular Biology Organization fellowship ALTF 131-1996 and by a visitors grant (B81.667) from the Dutch Foundation for Scientific Research (NWO). R.v.G. and H.v.A. were supported by the Dutch Foundation for Scientific Research (NWO). Financial support from the Lithuanian National Science and Study Foundation to L.V., V.C., R.K., and V.G. is also acknowledged.

REFERENCES

Agarwal, R., B. P. Krueger, G. D. Scholes, M. Yang, J. Yom, L. Mets, and G. R. Fleming. 2000. Ultrafast energy transfer in LHC-II revealed by three-pulse photon echo peak shift measurements. *J. Phys. Chem. B.* 104:2908–2918.

Bakker, J. G. C., R. van Grondelle, and W. T. F. den Hollander. 1983. Trapping, loss and annihilation of excitations in a photosynthetic system. II. Experiments with the purple bacteria *Rhodospirillum rubrum* and *Rhodopseudomonas capsulata. Biochim. Biophys. Acta.* 725:508–518.

Barzda, V., L. Mustardy, and G. Garab. 1994. Size dependency of circular dichroism in macroaggregates of photosynthetic pigment–protein complexes. *Biochemistry.* 33:10837–10841.

Barzda, V., G. Garab, V. Gulbinas, and L. Valkunas. 1995. Long distance migration of the excitation energy and fluorescence quenching mechanisms in chiral macroaggregates of LHCII. *In* Photosynthesis: From Light to Biosphere. P. Mathis, editor. Kluwer Academic Publishers, The Netherlands. 319–322.

Barzda, V., G. Garab, V. Gulbinas, and L. Valkunas. 1996. Evidence for long-range excitation energy migration in macroaggregates of the chlorophyll *a*/*b* light-harvesting antenna complexes. *Biochim. Biophys. Acta.* 1273:231–236.

Barzda, V., M. Vengris, F. Calkoen, R. van Grondelle, and H. van Amerongen. 1998. Reversible light-induced fluorescence quenching—an inherent property of LHCII. *In* Photosynthesis: Mechanisms and Effects, Vol. I. G. Garab, editor. Kluwer Academic Publishers, The Netherlands. 337–340.

Bassi, R., D. Sandona, and R. Croce. 1997. Novel aspects of chlorophyll *a*/*b*-binding proteins. *Physiol. Plant.* 100:769–779.

Becker, M., V. Nagarajan, and W. W. Parson. 1991. Properties of the excited-singlet states of bacteriochlorophyll *a* and bacteriopheophytin *a* in polar solvents. *J. Am. Chem. Soc.* 113:6840–6848.

Berens, S. J., J. Scheele, W. L. Butler, and D. Magde. 1985a. Time-resolved fluorescence studies of spinach chloroplasts. Evidence for the heterogeneous bipartite model. *Photochem. Photobiol.* 42:51–57.

Berens, S. J., J. Scheele, W. L. Butler, and D. Magde. 1985b. Kinetic modeling of time resolved fluorescence in spinach chloroplasts. *Photochem. Photobiol.* 42:59–68.

Bittner, T., K.-D. Irrgang, G. Renger, and M. R. Wasielewski. 1994. Ultrafast excitation energy transfer and exciton–exciton annihilation processes in isolated light harvesting complexes of photosystem II (LHCII) from spinach. *J. Phys. Chem.* 98:11821–11826.

Bittner, T., G. P. Wiederrecht, K.-D. Irrgang, G. Renger, and M. Wasielewski. 1995. Femtosecond transient absorption spectroscopy on the light-harvesting Chl *a*/*b* protein complex of Photosystem II at room temperature and 12 K. *Chem. Phys.* 194:311–322.

Boekema, E. J., B. Hankamer, D. Bald, J. Kruip, J. Nield, A. F. Boonstra, J. Barber, and M. Rögner. 1995. Supramolecular structure of the photosystem II complex from green plants and cyanobacteria. *Proc. Natl. Acad. Sci. U.S.A.* 92:175–179.

Boekema, E. J., H. van Roon, and J. P. Dekker. 1998. Specific association of photosystem II and light-harvesting complex II in partially solubilized photosystem II membranes. *FEBS Lett.* 424:95–99.

Boekema, E. J., H. van Roon, F. Calkoen, R. Bassi, and J. P. Dekker. 1999a. Multiple types of association of photosystem II and its light-harvesting antenna in partially solubilized photosystem II membranes. *Biochemistry.* 38:2233–2239.

Boekema, E. J., H. van Roon, J. F. L. van Breemen, and J. P. Dekker. 1999b. Supramolecular organization of photosystem II and its light-harvesting antenna in partially solubilized photosystem II membranes. *Eur. J. Biochem.* 266:444–452.

Boekema, E. J., J. F. L. van Breemen, H. van Roon, and J. P. Dekker. 2000. Arrangement of photosystem II supercomplexes in crystalline macrodomains within the thylakoid membranes of green plant chloroplasts. *J. Mol. Biol.* 301:1123–1133.

Breton, J., N. E. Geacintov, and C. S. Swenberg. 1979. Quenching of fluorescence by triplet excited states in chloroplasts. *Biochim. Biophys. Acta.* 548:616–635.

Bunde, A., and S. Havlin. 1991. Fractals and Disordered Systems. Springer Verlag, Berlin.

Burke, J. J., C. L. Ditto, and C. J. Arntzen. 1987. Involvement of the light-harvesting complex in cation regulation of excitation energy distribution in chloroplasts. *Arch. Biochem. Biophys.* 187:252–263.

Butler, W. L., D. Magde, and S. J. Berens. 1983. Fluorescence lifetimes in the bipartite model of the photosynthetic apparatus with alpha, beta heterogeneity in photosystem II. *Proc. Natl. Acad. Sci. U.S.A.* 80: 7510–7514.

Connelly, J. P., M. G. Müller, R. Bassi, R. Croce, and A. R. Holzwarth. 1997a. Femtosecond transient absorption study of carotenoid to chlorophyll energy transfer in light-harvesting complex II of photosystem II. *Biochemistry.* 36:281–287.

Connelly, J. P., M. G. Müller, M. Hucke, G. Gatzen, C. W. Mullineaux, A. V. Ruban, P. Horton, and A. R. Holzwarth. 1997b. Ultrafast spectroscopy of trimeric light-harvesting complex II from higher plants. *J. Phys. Chem. B.* 101:1902–1909.

Dau, H. 1994. Molecular mechanisms and quantitative models of variable photosystem II fluorescence. *Photochem. Photobiol.* 60:1–23.

Deinum, G., T. J. Aartsma, R. van Grondelle, and J. Amesz. 1989. Singlet–singlet annihilation measurements on the antenna of *Rhodospirillum rubrum* between 300 and 4K. *Biochim. Biophys. Acta.* 976:63–69.

Dekker, J. P., H. van Roon, and E. J. Boekema. 1999. Heptameric association of light-harvesting complex II trimers in partially solubilized photosystem II membranes. *FEBS Lett.* 449:211–214.

Den Hollander, W. T. F., J. G. C. Bakker, and R. van Grondelle. 1983. Trapping, loss and annihilation of excitations in a photosynthetic system. I. Theoretical aspects. *Biochim. Biophys. Acta.* 725:492–507.

Geacintov, N. E., J. Breton, C. E. Swenberg, and G. Paillotin. 1977. A single pulse picosecond laser study of excitation dynamics in chloroplasts. *Photochem. Photobiol.* 26:629–638.

Gillbro, T., A. Sandström, M. Spangfort, V. Sundström, and R. van Grondelle. 1988. Excitation energy annihilation in aggregates of chlorophyll *a*/*b* complexes. *Biochim. Biophys. Acta.* 934:369–374.

Gobets, B., I. H. M. van Stokkum, F. van Mourik, M. Rögner, J. Kruip, J. P. Dekker, and R. van Grondelle. 1998. Time-resolved fluorescence measurements of Photosystem I from *Synochocystis* sp. PCC 6803. *In* Photosynthesis: Mechanisms and Effects, Vol. I. G. Garab, editor. Kluwer Academic Publishers, The Netherlands. 571–574.

Gradinaru, C. C., S. Özdemir, D. Gülen, I. H. M. van Stokkum, R. van Grondelle, and H. van Amerongen. 1998. The flow of excitation in LHCII monomers. Implications for the structural model of the major plant antenna. *Biophys. J.* 75:3064–3077.

Horton, P., A. V. Ruban, and R. G. Walters. 1996. Regulation of light harvesting in green plants. *Ann. Rev. Plant Physiol. Plant Mol. Biol.* 47:655–684.

Ide, J. P., D. R. Klug, W. Kühlbrandt, L. B. Giorgi, and G. Porter. 1987. The state of detergent solubilised light-harvesting chlorophyll-*a*/*b* protein complex as monitored by picosecond time-resolved fluorescence and circular dichroism. *Biochim. Biophys. Acta.* 893:349–364.

Jansson, S. 1994. The light-harvesting chlorophyll *a*/*b*-binding proteins. *Biochim. Biophys. Acta.* 1184:1–19.

Jansson, S., H. Stefansson, U. Nystrom, P. Gustafsson, and P.-A. Albertsson. 1997. Antenna protein composition of PSI and PSII in thylakoid sub-domains. *Biochim. Biophys. Acta.* 1320:297–309.

Jennings, R. C., R. Bassi, F. M. Garlaschi, P. Dainese, and G. Zucchelli. 1993. Distribution of the chlorophyll spectral forms in the chlorophyll–protein complexes of photosystem II antenna. *Biochemistry.* 32:3203–3210.

Kleima, F. J., C. C. Gradinaru, F. Calkoen, I. H. M. van Stokkum, R. van Grondelle, and H. van Amerongen. 1997. Energy transfer in LHCII monomers at 77K studied by sub-picosecond transient absorption spectroscopy. *Biochemistry.* 36:15262–15268.

Kolubayev, T., N. E. Geacintov, G. Paillotin, and J. Breton. 1985. Domain size in chloroplasts and chlorophyll–protein complexes probed by fluorescence yield quenching induced by singlet-triplet exciton annihilation. *Biochim. Biophys. Acta.* 808:66–76.

Krauss, N., W.-D. Schubert, O. Klukas, P. Fromme, H. T. Witt, and W. Saenger. 1996. Photosystem I at 4 A resolution: a joint photosynthetic reaction center and core antenna system. *Nat. Struct. Biol.* 3:965–973.

Kudzmauskas, S., L. Valkunas, and A. Y. Borisov. 1983. A theory of excitation transfer in photosynthetic units. *J. Theor. Biol.* 105:13–23.

Kühlbrandt, W., D. N. Wang, and Y. Fujiyoshi. 1994. Atomic model of plant light-harvesting complex by electron crystallography. *Nature.* 367: 614–621.

Kwa, S. L. S., H. van Amerongen, S. Lin, J. P. Dekker, R. van Grondelle, and W. S. Struve. 1992a. Ultrafast energy transfer in LHC-II trimers from the Chl *a*/*b* light-harvesting antenna of photosystem II. *Biochim. Biophys. Acta.* 1102:202–212.

Kwa, S. L. S., F. G. Groeneveld, J. P. Dekker, R. van Grondelle, H. van Amerongen, S. Lin, and W. S. Struve. 1992b. Steady-state and time-resolved polarized light spectroscopy of the green plant light-harvesting complex II. *Biochim. Biophys. Acta.* 1101:143–146.

Lavergne, J., and H.-W. Trissl. 1995. Theory of fluorescence induction in photosystem II: derivation of analytical expressions in a model including exciton-radical-pair equilibrium and restricted energy transfer between photosynthetic units. *Biophys. J.* 68:2474–2492.

Mullineaux, C. W., A. A. Pascal, P. Horton, and A. Holzwarth. 1993. Excitation-energy quenching in aggregates of the LHCII chlorophyll-protein complex: a time-resolved fluorescence study. *Biochim. Biophys. Acta.* 1141:23–28.

Nordlund, T. M., and W. H. Knox. 1981. Lifetime of fluorescence from light-harvesting chlorophyll *a*/*b* proteins. Excitation intensity dependence. *Biophys. J.* 36:193–201.

Paillotin, G. 1976. Capture frequency of excitations and energy transfer between photosynthetic units in the photosystem II. *J. Theor. Biol.* 58:219–235.

Paillotin, G., C. E. Swenberg, J. Breton, and N. E. Geacintov. 1979. Analysis of picosecond laser-induced fluorescence phenomena in photosynthetic membranes utilizing a Master equation approach. *Biophys. J.* 25:513–534.

Paillotin, G., N. E. Geacintov, and J. Breton. 1983. A master equation theory of fluorescence induction, photochemical yield, and

singlet–triplet exciton quenching in photosynthetic systems. *Biophys. J.* 44:65–77.

Pålsson, L. O., M. D. Spangfort, V. Gulbinas, and T. Gillbro. 1994. Ultrafast chlorophyll *b*–chlorophyll *a* excitation energy transfer in the isolated light harvesting complex, LHCII, of green plants. Implications for the organisation of chlorophylls. *FEBS Lett.* 339:134–138.

Pearlstein, R. M. 1982. Excitation migration and trapping in photosynthesis. *Photochem. Photobiol.* 35:835–844.

Peterman, E. J. G., R. Monshouwer, I. H. M. van Stokkum, R. van Grondelle, and H. van Amerongen. 1997. Ultrafast singlet excitation transfer from carotenoids to chlorophylls via different pathways in light-harvesting complex II of higher plants. *Chem. Phys. Lett.* 264: 279–284.

Roelofs, T. A., C.-H. Lee, and A. R. Holzwarth. 1992. Global target analysis of picosecond chlorophyll fluorescence kinetics from pea chloroplasts. *Biophys. J.* 61:1147–1163.

Savikhin, S., H. van Amerongen, S. L. S. Kwa, R. van Grondelle, and W. S. Struve. 1994. Low-temperature energy transfer in LHC-II trimers from the Chl *a*/*b* light-harvesting antenna of photosystem II. *Biophys. J.* 66:1597–1603.

Savikhin, S., W. Xu, V. Soukoulis, P. R. Chitnis, W. S. Struve. 1999. Ultrafast primary processes in photosystem I of the cyanobacterium *Synochocystis* sp. PCC 6803. *Biophys. J.* 76:3278–3288.

Schödel, R., F. Hillmann, T. Schrötter, J. Voigt, K.-D. Irrgang, and G. Renger. 1996. Kinetics of excited states of pigment clusters in solubilized light-harvesting complex II—photon density-dependent fluorescence yield and transmittance. *Biophys. J.* 71:3370–3380.

Simidjiev, I., V. Barzda, L. Mustardy, and G. Garab. 1997. Isolation of lamellar aggregates of the light-harvesting chlorophyll *a*/*b* complex of photosystem II with long-range chiral order and structural flexibility. *Anal. Biochem.* 250:169–175.

Somsen, O. J. G., F. van Mourik, R. van Grondelle, and L. Valkunas. 1994. Energy migration and trapping in a spectrally and spatially inhomogeneous light-harvesting antenna. *Biophys. J.* 66:1580–1596.

Somsen, O. J. G., L. Valkunas, and R. van Grondelle. 1996. A perturbed two-level model for exciton trapping in small photosynthetic systems. *Biophys. J.* 70:669–683.

Sonneveld, A., H. Rademaker, and L. N. M. Duysens. 1979. Chlorophyll *a* fluorescence as a monitor of nanosecond reduction of the photooxidized primary donor P-680$^+$ of photosystem II. *Biochim. Biophys. Acta.* 548: 536–551.

Sonneveld, A., H. Rademaker, and L. N. M. Duysens. 1980. Transfer and trapping of excitation energy in photosystem II as studied by chlorophyll a_2 fluorescence quenching by dinitrobenzene and carotenoid triplet. The matrix model. *Biochim. Biophys. Acta.* 593:272–289.

Suna, A. 1970. Kinematics of exciton–exciton annihilation in molecular crystals. BV1:1716–1739.

Valkunas, L. 1986. Influence of structural heterogeneity on energy migration in photosynthesis. *Laser Chem.* 6:253–267.

Valkunas, L., V. Liuolia, and A. Freiberg. 1991. Picosecond processes in chromatofores at various excitation intensities. *Photosynth. Res.* 27: 83–95.

Valkunas, L., N. E. Geacintov, and L. L. France. 1992a. Fluorescence induction in green plants revisited. Origin of variabilities in sigmoidicities on different time scales of irradiation. *J. Luminesc.* 51:67–78.

Valkunas, L., F. van Mourik, and R. van Grondelle. 1992b. On the role of spectral and spatial antenna inhomogeneity in the process of excitation energy trapping in photosynthesis. *J. Photochem. Photobiol.* B-15: 159–170.

Valkunas, L., G. Trinkunas, V. Liuolia, and R. van Grondelle. 1995. Nonlinear annihilation of excitations in photosynthetic systems. *Biophys. J.* 69:1117–1129.

Valkunas, L., E. Akesson, T. Pullerits, and V. Sundström. 1996. Energy migration in the light-harvesting antenna of the photosynthetic bacterium *Rhodospirillum rubrum* studied by time-resolved excitation annihilation at 77 K. *Biophys. J.* 70:2373–2379.

Valkunas, L., G. Trinkunas, and V. Liuolia. 1999. Exciton annihilation in molecular aggregates. *In* Resonance Energy Transfer. D. Andrews, and A. Demidov, editors. John Wiley and Sons, Chichester, U.K. 244–307.

Van Amerongen, H., L. Valkunas, and R. van Grondelle. 2000. Photosynthetic Excitons. World Scientific Publishers, Singapore.

Van Grondelle, R. 1985. Excitation energy transfer, trapping and annihilation in photosynthetic systems. *Biochim. Biophys. Acta.* 811:147–195.

Van Grondelle, R., J. P. Dekker, T. Gillbro, and V. Sundström. 1994. Energy transfer and trapping in photosynthesis. *Biochim. Biophys. Acta.* 1187:1–65.

Vasil'ev, S., K.-D. Irrgang, T. Schrötter, A. Bergmann, H.-J. Eichler, and G. Renger. 1997. Quenching of chlorophyll *a* fluorescence in the aggregates of LHCII: steady state fluorescence and picosecond relaxation kinetics. *Biochemistry.* 36:7503–7512.

Visser, H. M., F. J. Kleima, I. H. M. van Stokkum, R. van Grondelle, and H. van Amerongen. 1996. Probing the many energy-transfer processes in the photosynthetic light-harvesting complex II at 77K using energy-selective sub-picosecond transient absorption spectroscopy. *Chem. Phys.* 210:297–312.

Visser, H. M., F. J. Kleima, I. H. M. van Stokkum, R. van Grondelle, and H. van Amerongen. 1997. Probing the many energy-transfer processes in the photosynthetic light-harvesting complex II at 77K using energy-selective sub-picosecond transient absorption spectroscopy. *Chemical Physics* 215:299 (erratum).

Wulf, K., and H.-W. Trissl. 1996. Competition between annihilation and trapping leads to strongly reduced yields of photochemistry under ps-flash excitation. *Photosynth. Res.* 48:255–262.